International Forum of Allergy & Rhinology

IFAR: International Forum of Allergy & Rhinology

ORIGINAL ARTICLE OPEN ACCESS

Selective PAR2 Inhibition Attenuates HDM-Induced Th1/Th2 Responses in Human Epithelial and Murine Models of Allergic Rhinitis and Asthma

Miran Kang[1] | Yohan Seo[2,3] | Ju Hee Seo[1] | Yeonsu Jeong[4] | Hyejin Jeon[2] | Su-Myeong Jang[2] | Chang-Hoon Kim[1,5] | Wan Namkung[2] | Hyung-Ju Cho[1,5,6]

[1]Department of Otorhinolaryngology, Yonsei University College of Medicine, Seoul, South Korea | [2]College of Pharmacy, Yonsei Institute of Pharmaceutical Science, Yonsei University, Incheon, South Korea | [3]Department of Bio-Nanomaterials, Bio Campus of Korea Polytechnics, Nonsan, South Korea | [4]Department of Otorhinolaryngology–Head and Neck Surgery, Chung-Ang University College of Medicine, Seoul, South Korea | [5]The Airway Mucus Institute, Yonsei University College of Medicine, Seoul, South Korea | [6]Graduate School of Medical Science, Brain Korea 21 Project, Yonsei University College of Medicine, Seoul, South Korea

Correspondence: Wan Namkung (wnamkung@yonsei.ac.kr) | Hyung-Ju Cho (hyungjucho@yuhs.ac)

Received: 2 February 2025 | **Revised:** 9 May 2025 | **Accepted:** 8 June 2025

Funding: This study was supported by the "Team Science Award" of Yonsei University College of Medicine (6-2021-0005). This work was also supported by National Research Foundation of Korea (NRF) grants funded by the Korean government (MSIT) (No. RS-2023-00220853, NRF-2021R1A2C2010811, and NRF-2022M3A9J4079468 to H.J. Cho, and NRF-2018R1A6A1A03023718 to W. Namkung).

Keywords: allergic airway inflammation | protease-activated receptor 2 | punicalagin | rhinitis and asthma | Th1/Th2 responses

ABSTRACT

Background: Allergic rhinitis (AR) and asthma are involved in complex interactions between Th1 and Th2 inflammatory pathways. House dust mite (HDM) activates protease-activated receptor 2 (PAR2) to trigger inflammatory responses, but current treatments often provide inadequate control.

Objective: This study aimed to investigate the effects of selective PAR2 inhibition on Th1 and Th2 responses in human nasal epithelial (HNE) cells and murine models of AR and asthma.

Methods: We examined the effects of selective PAR2 inhibition using primary HNE cells and HDM-induced mouse models (PAR2-wild-type [PAR2-wt] and knockout [PAR2-ko]). Analyses included inflammatory signaling pathways, cytokine profiles, airway responses, histopathology, and transcriptomics.

Results: In HNE cells, PAR2 inhibition suppressed Th2 (interleukin [IL]-33, TSLP) and Th1 (TNF-α, IL-6) inflammatory cytokines while inhibiting calcium mobilization and ERK/NF-κB signaling cascades. In PAR2-wt mice, treatment with the PAR2 inhibitor reduced HDM-specific Immunoglobulin E (IgE), airway hyperresponsiveness, and allergic inflammation in both nasal and bronchial tissues, matching the anti-inflammatory profile of PAR2-ko mice. Bulk RNA sequencing confirmed comprehensive suppression of inflammatory gene expression.

Conclusions: Selective PAR2 inhibition effectively attenuates HDM-induced allergic inflammation by modulation of Th1 and Th2 pathways in human airway epithelium and murine models. We suggest that PAR2 can be a possible target for AR and asthma.

Wan Namkung and Hyung-Ju Cho contributed equally to this work.

1 | Introduction

Allergic airway diseases, such as allergic rhinitis (AR) and allergic asthma, are not isolated conditions but rather part of a complex interplay between Th1 and Th2 immune responses [1]. While traditionally viewed as Th2-dominant conditions, emerging evidence suggests a more nuanced inflammatory pattern. AR manifests as sneezing, rhinorrhea, and nasal congestion [2–4], whereas allergic asthma presents with airway narrowing, mucus hypersecretion, and respiratory distress [5]. Despite their distinct symptoms, both conditions share underlying inflammatory mechanisms characterized by airway hyperresponsiveness (AHR) and dysregulated immune responses.

House dust mite (HDM) emerges as a pivotal allergen in these respiratory conditions through its unique ability to activate Th1 and Th2 pathways. HDM's protease components specifically target protease-activated receptor 2 (PAR2), a seven-transmembrane G-protein-coupled receptor that serves as a crucial immunological sentinel [6]. When HDM proteases cleave PAR2's N-terminus, the exposed tethered ligand binds to the receptor's extracellular loop 2, initiating a cascade of inflammatory responses [7]. PAR2's strategic expression across multiple cell types—including airway epithelial cells, immune cells (mast cells, macrophages, dendritic cells, T cells), and structural cells (fibroblasts, myocytes, sensory neurons)—positions it as a master regulator of both Th1 and Th2 responses [8].

The activation of PAR2 triggers parallel inflammatory cascades: the NF-κB pathway driving Th1 responses and ERK 1/2 signaling influencing Th2 responses [9, 10]. Additionally, PAR2 mobilizes cytosolic Ca^{2+} through CRAC channels (encoded by STIM1 and Orai1), orchestrating a complex inflammatory response that includes both Th1 cytokines (such as TNF-α) and Th2 mediators (including IL-33 and TSLP) [11]. This dual activation pattern is particularly relevant in allergic airways, where PAR2 overexpression in nasal mucosa correlates with disease severity [12–15].

Despite extensive research into PAR2 antagonism, the field lacks a clinically viable inhibitor that can effectively modulate Th1 and Th2 responses. Punicalagin (PCG), recently identified as a selective PAR2 inhibitor, shows promising potential [10, 16]. Although previously known for its antioxidant properties, we discovered PCG's selective inhibition of PAR2 in human airway epithelium affects both Th1 and Th2 pathways. This study aims to validate PCG's therapeutic potential in HDM-induced allergic airways by examining its dual modulatory effects on Th1 and Th2 responses while elucidating the underlying mechanisms of allergic airway inflammation.

2 | Methods

2.1 | Animals

Experiments were performed with the approval of the Institutional Animal Care and Use Committee of Yonsei University (2018-0168). Sex was not considered as a biological variable. PAR2-transgenic mice were provided by the Korea Research Institute of Bioscience and Biotechnology. Animals were reared in accordance with the environmental stipulations outlined by the Department of Laboratory Animal Resources, Yonsei Biomedical Research Institute, Yonsei University College of Medicine. Experiments were conducted with PAR2 wild-type (PAR2-wt) and knockout (PAR2-ko) C57BL/6 mice produced by mating the parental generation. The genotypes of the offspring were confirmed by PCR and DNA electrophoresis with Mupid-exU (Takara Bio, Seoul, Korea), which showed the characteristic bands at 345 and 198 bp for PAR2-wt and PAR2-ko mice, respectively (Table S1).

2.2 | Mouse Modeling of AR and Asthma

The mouse model was developed in accordance with a previously published method [17]. In brief, AR and asthma were simultaneously induced in 8-week-old male PAR2-wt and PAR2-ko mice by administering three sensitization doses and four challenge doses with the mice under isoflurane sedation to ensure proper delivery to the lower airway (Ifrane, Hana Pharm, Gyeonggi, Korea). For sensitization, a 200 μL total volume of HDM (100 μg/mL; Greer Laboratories Inc, NC, USA) and Alum (2 mg/mL; Thermo Scientific, MA, USA) in phosphate-buffered saline (PBS) was injected intraperitoneally on Days 0, 7, and 14. Seven days after the last sensitization dose, a 50 μL challenge dose of PBS (control) or 1 mg/mL HDM in PBS was injected intranasally for four consecutive days (Days 21–24). PCG was provided by Prof. Namkung and administered intraperitoneally (10 mg/kg, 50 μL) from Days 20 to 24 to determine the therapeutic effect of PAR2 inhibition. Mice were euthanized by CO_2 inhalation, and nasal and lung tissues were harvested for analysis.

2.3 | Measurement of AHR

AHR to inhaled methacholine was measured in the mouse model on Day 25 of the modeling protocol. Before measurement, the mice were acclimated to the test conditions for 2 weeks to prevent stress during measurement. After putting each mouse in the chamber, AHR to inhaled PBS (Lonza, Basel, Switzerland) or methacholine (Sigma, Kanagawa, Japan) was measured. Methacholine (0, 6.25, 12.5, 25, and 50 mg/mL) was administered sequentially from low to high concentrations. At the end of one cycle of measurement, the inside of the machine was cleaned before starting the next cycle.

2.4 | Immunoglobulin E (IgE) Level Measurement by Enzyme-Linked Immunosorbent Assay (ELISA)

On Day 26 of the modeling protocol, blood was collected from the mice, the serum was separated, and serum IgE levels were ascertained by ELISA for total IgE and HDM-specific IgE. Total IgE was measured according to the protocol of the mouse IgE uncoated ELISA kit (Invitrogen, MA, USA). HDM-specific IgE ELISA was measured according to the protocol of the mouse serum anti-HDM IgE antibody assay kit (Chondrex, WA, USA).

2.5 | Histopathology

After sacrifice, the mice were perfused with PBS, and the head and lungs were harvested and fixed in 4% paraformaldehyde (PFA) (Biosesang, Gyeonggi, Korea) for 4 days. Decalcification

was performed by placing the samples in 10% EDTA (Biosesang, Gyeonggi, Korea) for 20 days. Finally, the samples were fixed again with 4% PFA. The head, including the nasal cavity, and the lung tissues were sectioned and embedded in paraffin blocks, trimmed and sectioned in 4 μm slices, and mounted on slides. Hematoxylin and eosin (H&E) staining, periodic-acid-Schiff (PAS) staining, and Sirius red (SR) staining were performed, and the differences between treatment groups were observed. To quantify goblet cells and eosinophils in nasal tissues, we analyzed the posterior nasal cavity's turbinate mucosa at the middle turbinate level in coronal sections. Two independent investigators, blinded to the experimental groups, analyzed five nonoverlapping fields for each animal.

2.6 | Immunofluorescence

Sectioned slides were placed in xylene (Duksan, Gyeongju, Korea) and deparaffinized in 100%–70% ethanol (Duksan). Steaming antigen retrieval was performed for 40 min with epitope retrieval solution (IW-1100-1L, IHC-TeK). A circle was marked around the tissue using a PAP pen (IHC WORLD, Gyeonggi, Korea) to preserve the solution on the tissue during cooling. Endogenous peroxidase was inactivated with 3% peroxidase-blocking solution (DAKO, CA, USA). The slides were blocked with 5% bovine serum albumin (BSA; Sigma) for 1 h at room temperature and incubated with the primary antibody Muc5ac (1:500; Invitrogen, MA, USA) at 4°C overnight. The slides were then rinsed three times with 1× tris-buffered saline (TBS) and incubated with goat anti-mouse Alex 568 (1:500) for 30 min. The slides were mounted with Fluoromount with DAPI (F6057-20ML, Sigma), and confocal images were taken with a 40× lens on a Carl Zeiss LSM 700 microscope and processed using ZEN software.

2.7 | Bulk RNA Sequencing

The nasal mucosa and lung lobe of the mice were isolated for bulk RNA-seq. Tissue samples were rinsed gently in saline to remove as much blood as possible, placed in RNA later solution (Invitrogen, Carlsbad, CA), and stored at −20°C. Analyses were conducted one by one for each specimen in each group. The samples were sent to Macrogen (Seoul, Korea) for analysis of cytokines (*interleukin 4* [*Il-4*], *Il-5*, *Il-6*, *Il-10*, *Il-13*, *Il-17*, *Il-33*, and *interferon-gamma* [*Ifn-γ*]), goblet cell markers (*Muc5ac*, *Cst1*, *Spdef*, *Fetub*, *Tspan8*, *Agr2*, *Ifi35*, *Serpinb2*, and *Timp1*), chemokines (*Ccr5*, *Ccl2*, *Ccl11*, *Ccl20*, *Ccl24*, *Cxcr4*, and *Cxcl12*), signaling pathways (*Gata3*, *Tlr2*, *Tlr4*, *Mapk*, *Rela*, *phospho65*, *NF-κB*, *TNF*, *Pi3k-Akt*, *Egfr*, and *Jak-Stat*), ion channels (*Cftr*, *Soce*, and *ENaC-β*), and epithelial–mesenchymal transition (EMT) markers (*PD-L1*, *E-cadherin*, *vimentin*, and *Tgf-β*).

2.8 | Primary Human Nasal Epithelial (HNE) Cell Culture

This study was approved by the Institutional Review Board of Yonsei University College of Medicine (4-2021-0573) and all subjects provided informed consent. Sex was not considered as a biological variable. Primary HNE cells were obtained from nasal mucosal tissue. The harvested tissue was incubated in 5 mL 0.1% protease overnight at 4°C. Epithelial cells isolated by scraping were cultured in a 100 ø dish (Corning, NY, USA) for passages 0 and 1 and then in a Costar 3460 transwell 12 mm plate (Corning, ME, USA) for passage 2. The subculture medium used for passages 0 and 1 was a mixture of bronchial epithelial cell growth medium (BEGM) Bulletkit (Lonza, Basel, Switzerland), 150 mg/mL BSA (Sigma, MO, USA), and epidermal growth factor. Cell culture for passage 2 was performed using a filtered culture medium called +RA + BPE medium, which contained 150 mg/mL BSA in a 1:1 mixture of BEGM and Dulbecco's modified Eagle medium. After each passage, cells were removed from the plate with 0.25% trypsin-EDTA (Gibco, Seoul, Korea) and neutralized with trypsin neutralizing solution (Lonza, Basel, Switzerland) after 1–2 min. When the cells were full at passage 2, airway liquid interface culture was started by removal of the culture medium from the apical side of the cells. During 2 weeks of interface culture to allow full differentiation, only the basolateral side of the culture was filled with culture medium.

2.9 | Intracellular Calcium Measurement

Intracellular calcium levels were quantified using the calcium-sensitive fluorescent probe Fluo-4 NW (Invitrogen, Carlsbad, CA, USA), following the manufacturer's protocol. Briefly, differentiated NHE cells cultured on transwell 12 mm permeable supports (Corning, ME, USA) were washed twice with PBS and mounted onto a perfusion chamber. The cells were then incubated for 50 min with 300 μL assay buffer containing Fluo-4. Subsequently, the cells were treated with PCG for 10 min before stimulation with PAR2 agonists. The Fluo-4 fluorescence was measured using an inverted fluorescence microscope (Nikon, Tokyo, Japan) equipped with an excitation filter (488 nm), an emission filter (515 nm), a cooled charge-coupled device camera (Zyla sCMOS; Andor Technology, Belfast, UK), and image acquisition and analysis software (Meta Imaging Series 7.7; Molecular Devices, Biberach, Germany). PCG was dissolved in dimethyl sulfoxide solution (DMSO), and cells were treated with a final concentration of 0.1% DMSO.

2.10 | Western Blot and Immunoblotting

HNE cells were washed twice with PBS and lysed in cell lysis buffer [50 mM Tris–HCl (pH 7.4), 1% Nonidet P-40, 0.25% sodium deoxycholate, 150 mM NaCl, 1 mM EDTA, 1 mM Na3VO4, and protease inhibitor mixture] on ice. Whole-cell lysates were centrifuged at 13,000 × *g* for 20 min at 4°C. Protein extracts were separated on 4%–12% Tris-glycine precast gels (Komabiotech, Seoul, Korea) and transferred to PVDF membranes (Millipore, Billerica, MA, USA). Membranes were blocked with 3% BSA in TBST (0.1% Tween 20) for 1 h and then incubated with anti-ERK1/2 (9101, 1:1000; Cell signaling, Danvers, MA, USA), anti-p-ERK1/2 (9102, 1:1000; Cell Signaling), anti-P65 (sc-8008, 1:1000; Santa Cruz Biotechnology, Santa Cruz, CA, USA), and anti-p-P65 (sc-136548, 1:1000; Santa Cruz Biotechnology). After three washes with TBST, the membranes were incubated at room temperature for 1 h with the appropriate HRP-conjugated secondary antibody. Protein levels were detected with an ECL

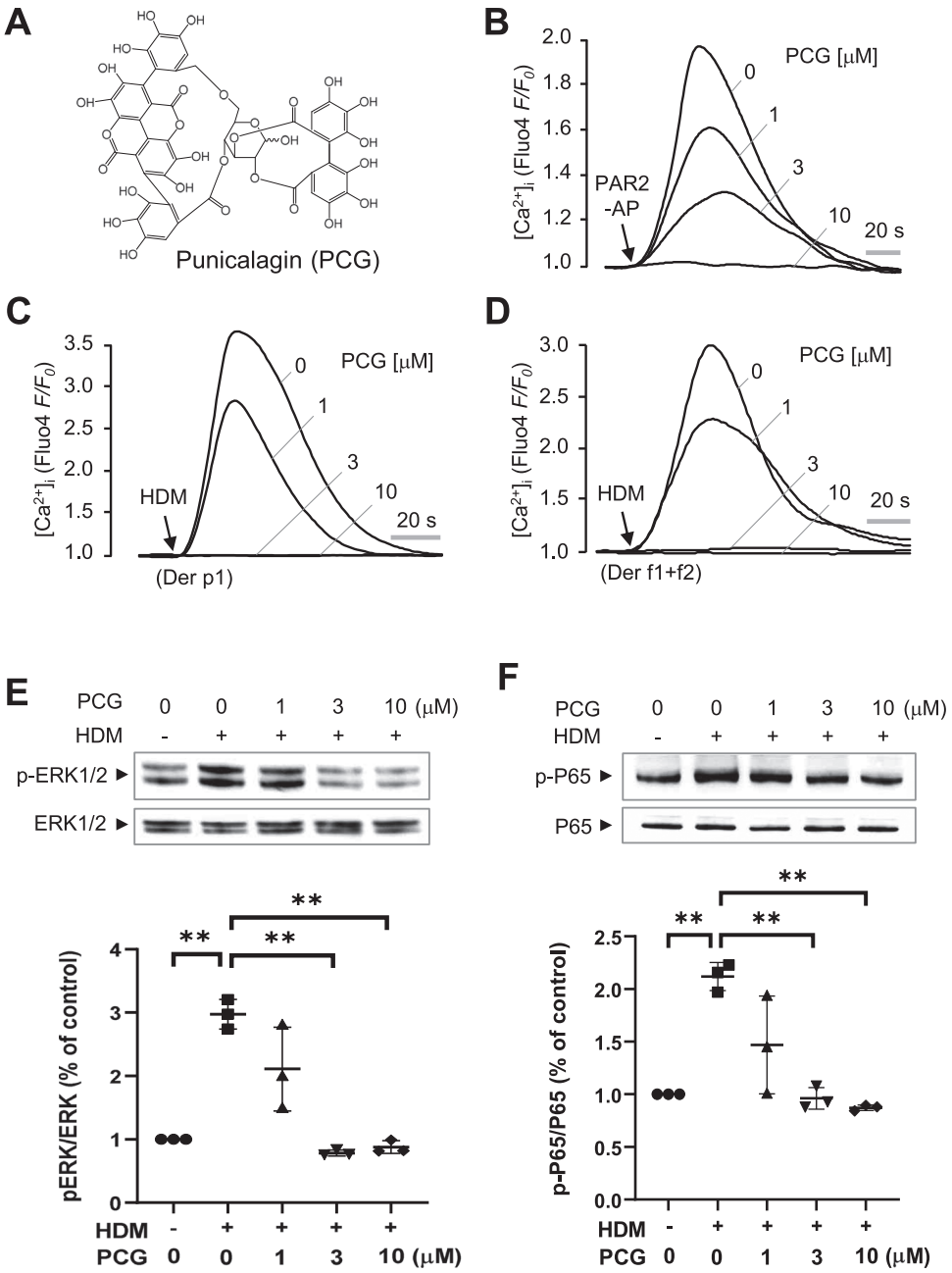

FIGURE 1 | Inhibitory effect of punicalagin on PAR2 in human nasal epithelial cells. (A) Chemical structure of PCG. (B–D) Intracellular calcium signaling induced by PAR2-AP (B), Der p1 house dust mite (C), and Der f1 + Der f2 house dust mite (D). The increases in intracellular calcium concentration induced by the PAR2 agonists were inhibited by the indicated concentrations of PCG. (E and F) Western blot analysis of phospho-ERK1/2 (p-ERK1/2), total ERK1/2 (t-ERK1/2), phospho-P65 (p-65), and total P65 (t-p65) in human nasal epithelial cells. The indicated concentrations of PCG were applied 30 min prior to PAR2 activation by HDM (mean ± S.E., $n = 3$). $^{**}p < 0.01$.

reagent using the FUSION SOLO imaging system (Vilber Lourmat, Marne-la-Vallée, France). ImageJ was used to quantify band intensity.

2.11 | Multiplex Assay

After HNE cells were differentiated, +RA + BPE medium was applied to the apical and basolateral chambers to hold the zero point for 12 h. In the apical and basolateral baths, PCG was applied at various concentrations for 30 min, and 100 μL HDM extract was then applied for 6 h. Samples from each chamber were collected and entrusted to KomaBiotech Inc. for cytokine analysis using the Human XL Cytokine Premixed Kit (R&D, catalog number FCSTM18).

2.12 | Statistical Analysis

All data were collected in three or more replicate experiments. Statistical comparisons were performed by Student's *t*-test or one-way ANOVA using GraphPad Prism 8.0 (San Diego, CA, USA).

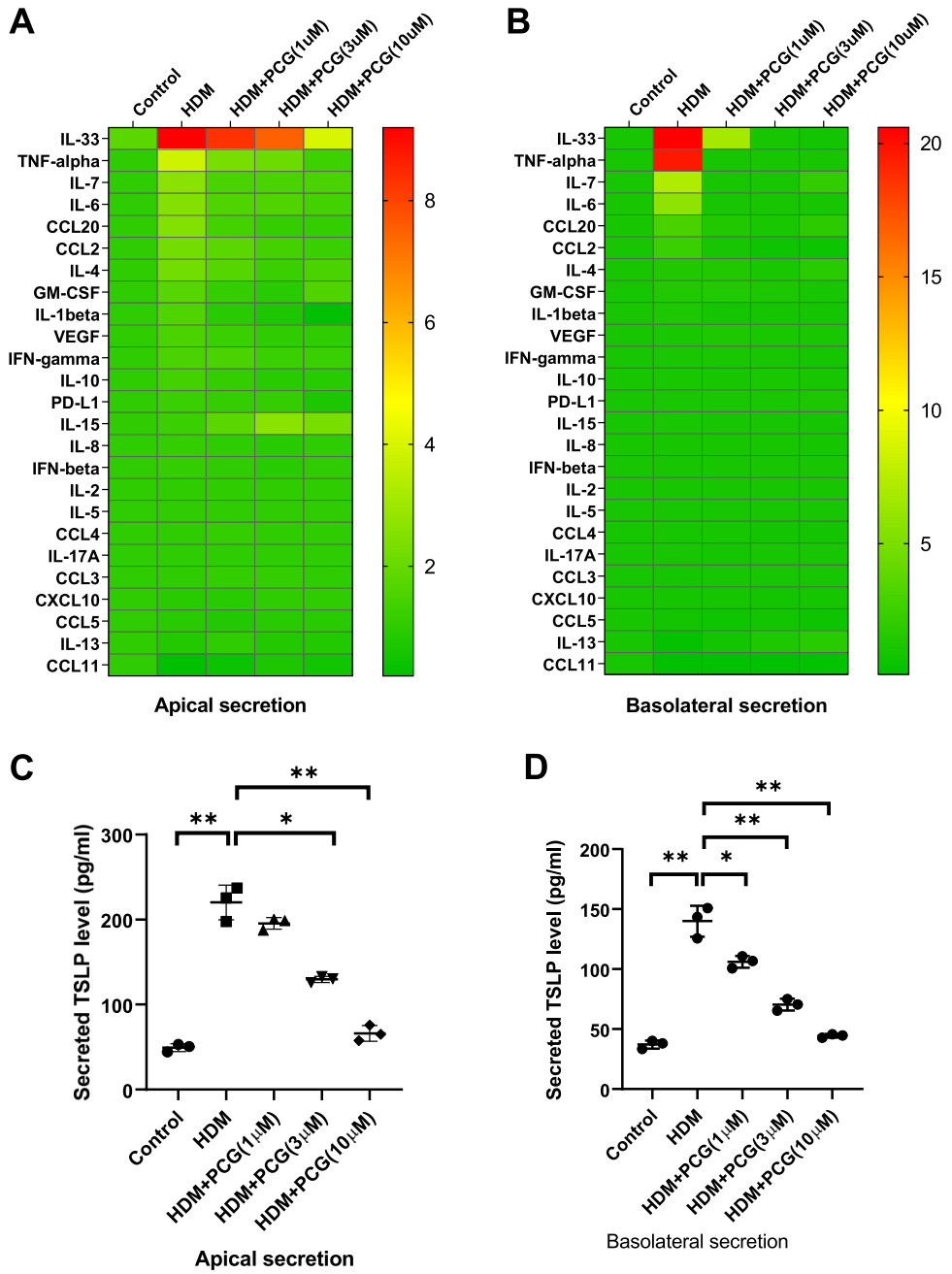

FIGURE 2 | PAR2-mediated cytokine secretion and inhibitory effect of punicalagin in human nasal epithelial cells. (A) Cytokine profiles in the apical secretion measured by multiplex cytokine assay. (B) Cytokine profiles in the basolateral secretion measured by multiplex cytokine assay. (C) TSLP protein level in apical secretion measured by ELISA after stimulation with HDM with or without PCG. (D) TSLP protein level in basolateral secretion measured by ELISA after stimulation with HDM with or without PCG. HDM, house dust mite; Ifn-γ, interferon-gamma; IL, interleukin. $^{*}p < 0.05$; $^{**}p < 0.01$.

p values less than 0.05 were considered significant ($^{*}p < 0.05$, $^{**}p < 0.01$, and $^{***}p < 0.001$).

3 | Results

3.1 | PCG Selectively Inhibits PAR2-Mediated Signaling in Human Airway Epithelium

PCG fully inhibited the elevation of intracellular calcium levels in HNE cells caused by PAR2-activating peptide (PAR2-AP) or HDM in a dose-dependent manner (Figure 1A–D). To elucidate the effect of PCG on key signaling cascades in PAR2-mediated inflammatory processes, changes in phosphorylated ERK (p-ERK) and phosphorylated p65 (p-p65) were examined in HNE cells. Stimulation with HDM augmented the phosphorylation of ERK1/2, and pretreatment with PCG blocked this phosphorylation in a dose-dependent manner. At a concentration of 3 μM, PCG almost completely abrogated the PAR2-mediated phosphorylation of ERK1/2 (Figure 1E). HDM also elevated p65 phosphorylation, which was inhibited by PCG in a dose-dependent manner (Figure 1F). In HNE cells, HDM-induced

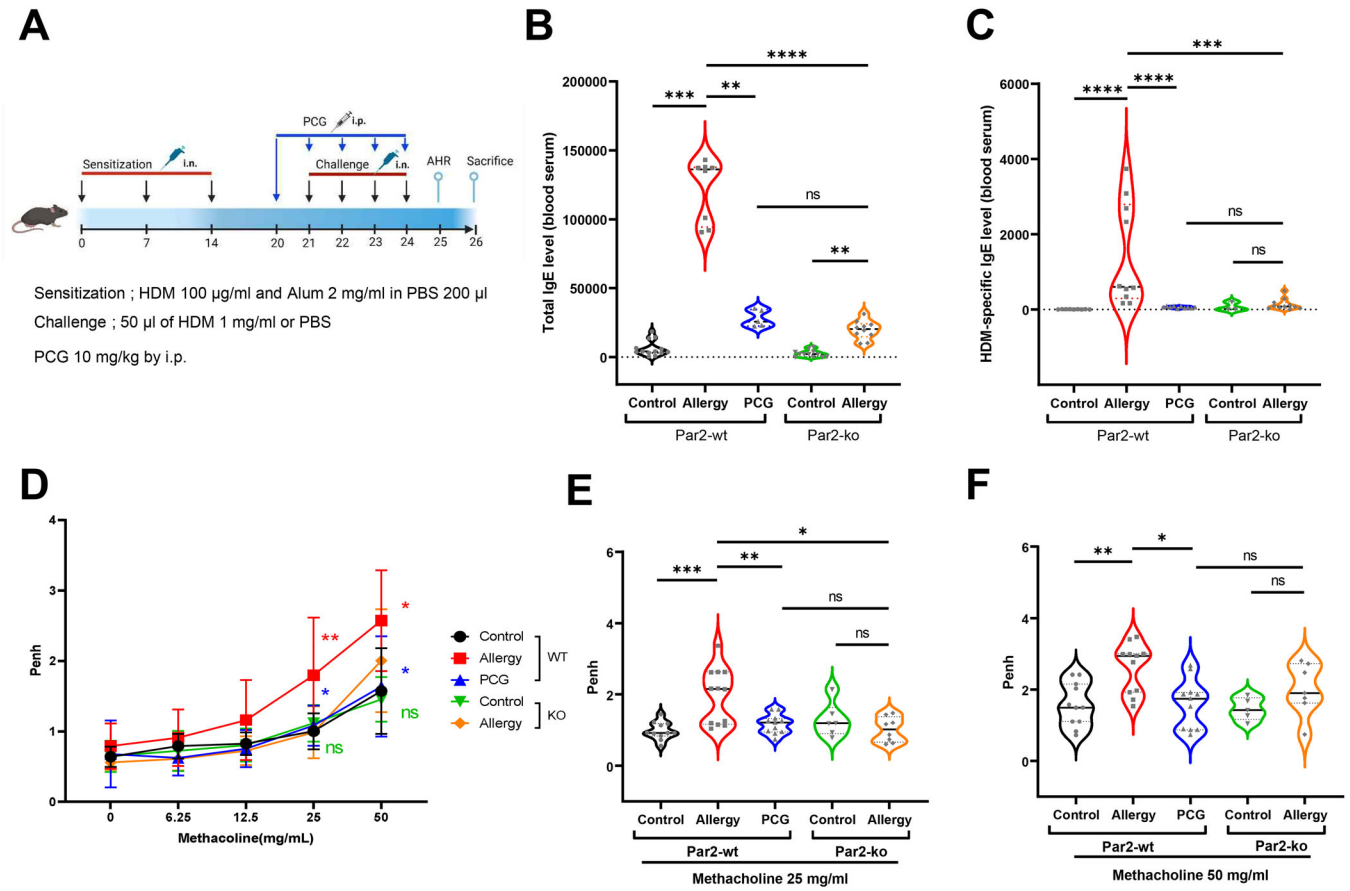

FIGURE 3 | Experimental protocol of the allergic rhinitis and asthma mouse model. (A) Mice were sensitized three times intraperitoneally and challenged intranasally under anesthesia for four consecutive days starting 1 week after sensitization. PCG was pretreated intraperitoneally. (B and C) Levels of total and HDM-specific IgE in serum in PAR2-wt and PAR2-ko mice. In PAR2-wt mice, the allergy group showed increased total IgE (B) and HDM-specific IgE (C), which were suppressed in the PCG group. In PAR2-ko mice, the allergy group showed similar total IgE (B) and HDM-specific HDM (C) levels to the PCG group of PAR2-wt mice. (D–F) Measurement of airway hyperresponsiveness (Penh) by methacholine stimulation test in the asthma model. (D) Plots showing Penh levels after dose-dependent methacholine stimulation in all groups. The increase of Penh induced by 25 mg/mL (E) or 50 mg/mL (F) methacholine was suppressed by PCG in PAR2-wt mice. The allergy group of PAR2-ko mice showed no difference in Penh level compared to the control group of PAR2-ko mice or the PCG group of PAR2-wt mice. PAR2, protease-activated receptor 2; PAR2-ko, PAR2 knockout; PAR2-wt, PAR2 wild-type. $^{*}p < 0.05$; $^{**}p < 0.01$; $^{***}p < 0.001$; $^{****}p < 0.0001$; ns $p > 0.05$.

phosphorylation of ERK1/2 and p65 was significantly blocked by AZ3451, a potent and selective PAR2 antagonist (Figure S1). These findings suggest that PCG suppresses the PAR2-mediated ERK1/2 and NF-κB signaling cascades, which are implicated in airway inflammation.

3.2 | PCG Modulates Both Th1 and Th2 Cytokine Production in HNE Cell

To find essential cytokines secreted from epithelial cells after HDM stimulation, we performed multiplex cytokine assays of the apical and basolateral secretions of HNE cells. The most significant cytokine secreted from HNE cells was IL-33, followed by TNF-α, IL-7, and IL-6 on the apical and basolateral sides (Figure 2A,B). The HDM-induced cytokine secretion was suppressed by PCG in a dose-dependent manner starting from 1 μM. The protein level of TSLP was measured separately by ELISA because TSLP was not involved in the multiplex cytokine panel. HDM stimulation induced TSLP secretion after 1 h on the basolateral side and after 6 h on the apical side of HNE cells. PCG suppressed TSLP secretion starting at concentrations of 3 μM on the apical side and 1 μM on the basolateral side (Figure 2C,D). These results indicate that TSLP secretion from epithelial cells is mediated through the PAR2 signaling pathway.

3.3 | PCG Suppresses HDM-Induced IgE Production in Allergic Murine Models

Serum total and HDM-specific IgE levels were measured by ELISA to confirm the phenotypes of the murine AR and asthma model (Figure 3A). In PAR2-wt mice, the allergy group showed increased total and HDM-specific serum IgE levels, whereas the PCG group showed suppression of these levels compared with the allergy group. In PAR2-ko mice, serum total and HDM-specific IgE levels in the allergy group were elevated compared with those in the control group, but they were significantly lower than those in the PAR2-wt allergy group. The total and HDM-specific serum

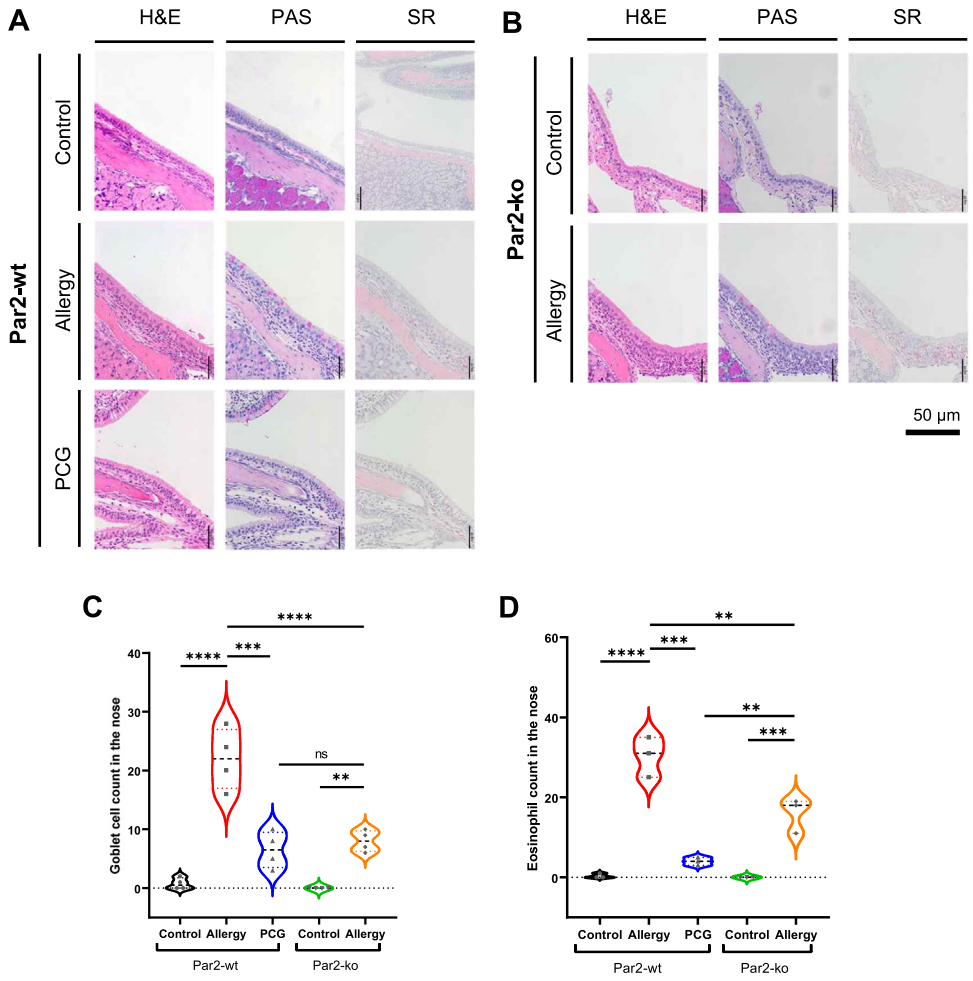

FIGURE 4 | Histopathology of nasal epithelium in the mouse model. (A) In PAR2-wt mice, the allergy group showed increased goblet cells by PAS staining and increased eosinophils by Sirius red (SR) staining compared with the control and PCG groups. (B) The number of goblet cells in the PAR2-ko allergy group was similar to that in the PAR2-wt PCG group but higher than that in the PAR2-ko control group. (C) Comparison of goblet cell numbers among groups in PAR2-wt and PAR2-ko mice. The PAR2-wt PCG group and the PAR2-ko allergy group showed significantly lower goblet cell numbers than the PAR2-wt allergy group. (D) Comparison of eosinophil numbers among groups in PAR2-wt and PAR2-ko mice. The PAR2-wt PCG group and the PAR2-ko allergy group showed significantly lower eosinophil numbers than the PAR2-wt allergy group. H&E, hematoxylin and eosin; PAR2, protease-activated receptor 2; PAR2-ko, PAR2 knockout; PAR2-wt, PAR2 wild-type; PAS, periodic-acid-Schiff; PCG, punicalagin. *$p < 0.05$; **$p < 0.01$; ***$p < 0.001$; ****$p < 0.0001$; ns $p > 0.05$.

IgE levels in the PAR2-ko allergy group were similar to those in the PAR2-wt PCG group (Figure 3B,C).

3.4 | PCG Attenuates Airway Hyperresponsiveness in HDM-Induced Allergic Airways

AHR to increasing doses of methacholine was expressed in enhanced pause (Penh) values. The Penh values showed dose-dependent elevation after methacholine stimulation in all groups. The PAR2-wt allergy group displayed higher levels of AHR than the other groups.

In PAR2-wt mice, the Penh values induced by 25 and 50 mg/mL methacholine were higher in the allergy group than in the control group and lower in the PCG group than in the allergy group. In PAR2-ko mice, the corresponding values in the allergy group were not different from those in the control group (Figure 3D–F).

3.5 | PCG Reduces Allergic Inflammatory Cell Infiltration and Tissue Remodeling

In PAR2-wt mice, the allergy group showed increased numbers of PAS-positive goblet cells compared with the control and PCG groups in both nasal (Figure 4A,C) and bronchial (Figure 5A,C) epithelium. The allergy group of PAR2-wt mice showed increased numbers of eosinophils compared with the control and PCG groups in both nasal (Figure 4A,D) and bronchial (Figure 5A,D) epithelium, confirming allergic inflammation in the tissues.

The numbers of goblet cells and eosinophils in the PAR2-ko allergy group were higher than those in the PAR2-ko control group but lower than those in the PAR2-wt allergy group, in both

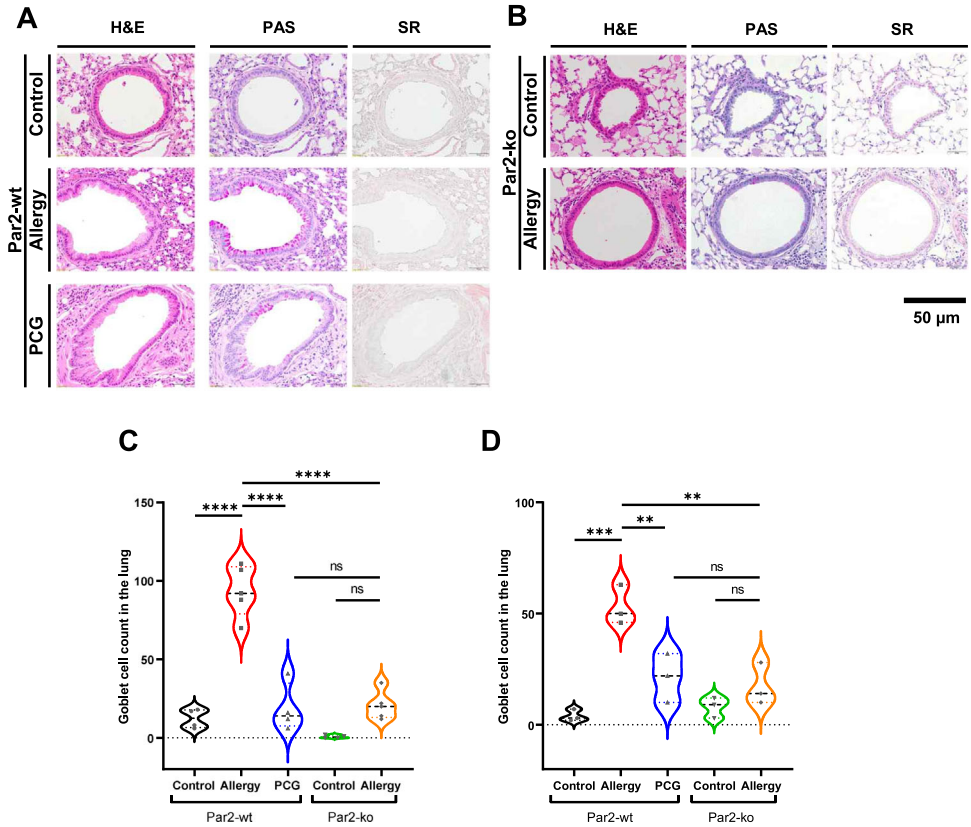

FIGURE 5 | Histopathology of bronchial epithelium in the mouse model. (A) In PAR2-wt mice, the allergy group showed thickened bronchial epithelium by H&E staining, increased goblet cells by PAS staining, and increased eosinophils by Sirius red (SR) staining compared with the control and PCG groups. (B) In PAR2-ko mice, the control and allergy groups showed low numbers of goblet cells and eosinophils. (C) Comparison of goblet cell numbers among groups in PAR2-wt and PAR2-ko mice. The PAR2-wt PCG group and the PAR2-ko allergy group showed significantly lower goblet cell numbers than the PAR2-wt allergy group. (D) Comparison of eosinophil numbers among groups in PAR2-wt and PAR2-ko mice. The PAR2-wt PCG group and the PAR2-ko allergy group showed significantly lower eosinophil numbers than the PAR2-wt allergy group. H&E, hematoxylin and eosin; PAR2, protease-activated receptor 2; PAR2-ko, PAR2 knockout; PAR2-wt, PAR2 wild-type; PAS, periodic-acid-Schiff; PCG, punicalagin. Scale bar, 50 μm; $^{*}p < 0.05$; $^{**}p < 0.01$; $^{***}p < 0.001$; $^{****}p < 0.0001$; ns $p > 0.05$.

nasal (Figure 4B–D) and bronchial (Figure 5B–D) epithelium. The number of goblet cells was similar between the PAR2-ko allergy group and the PAR2-wt PCG group in both nasal (Figure 4C) and bronchial (Figure 5C) epithelium. Expression of the major secretory mucin Muc5ac was determined in nasal and bronchial epithelium by confocal microscopy (Figure 6). The PAR2-wt allergy group showed overexpression of Muc5ac, which was significantly suppressed in the PAR2-wt PCG group in both nasal (Figure 6A,E) and bronchial (Figure 6B,F) epithelium. In PAR2-ko mice, Muc5ac expression in the allergy group was similar to that in the control group in both nasal (Figure 6C) and bronchial (Figure 6D) epithelium. The Muc5ac expression in the PAR2-ko allergy group was similar to that in the PAR2-wt PCG group (Figure 6E,F).

3.6 | Transcriptomic Analysis Reveals PCG's Comprehensive Effects on Inflammatory Gene Expression

Bulk RNA-seq (Figure S2) was performed to determine the alteration of genes associated with PAR2 after PCG treatment or PAR2-ko in nasal (Figure 7A,B) and bronchial (Figure 7C,D) tissues. In nasal tissue, *Eif2s3y*, *Ddx3y*, *Uty*, *Kdm5d*, and *Serpina3e-ps* were the top five significantly suppressed genes after both PCG treatment (Figure 7A) and PAR2-ko (Figure 7B). In bronchial tissue, *Eif2s3y*, *Ddx3y*, *Uty*, *Kdm5d*, and *Gm42031* were the top five significantly suppressed genes after both PCG treatment (Figure 7C) and PAR2-ko (Figure 7D). These results suggest that PCG can specifically inhibit PAR2-mediated signaling pathways, implying potential therapeutic effects for PAR2-related diseases.

To compare gene expression among treatment groups, we selected major genes related to allergic inflammation, such as Th2 cytokines, goblet cell markers, chemokines, signaling pathways, ion channels, and EMT (Figure 8). In the nasal and lung tissues of PAR2-wt mice, the PCG group showed lower expression of most genes compared with the allergy group. In PAR2-ko mice, although the gene expression in the allergy group was higher than that in the control group, it was still lower than that in the allergy group of PAR2-wt mice. These results imply that PAR2 is associated with the pathogenesis of allergic airway inflammation.

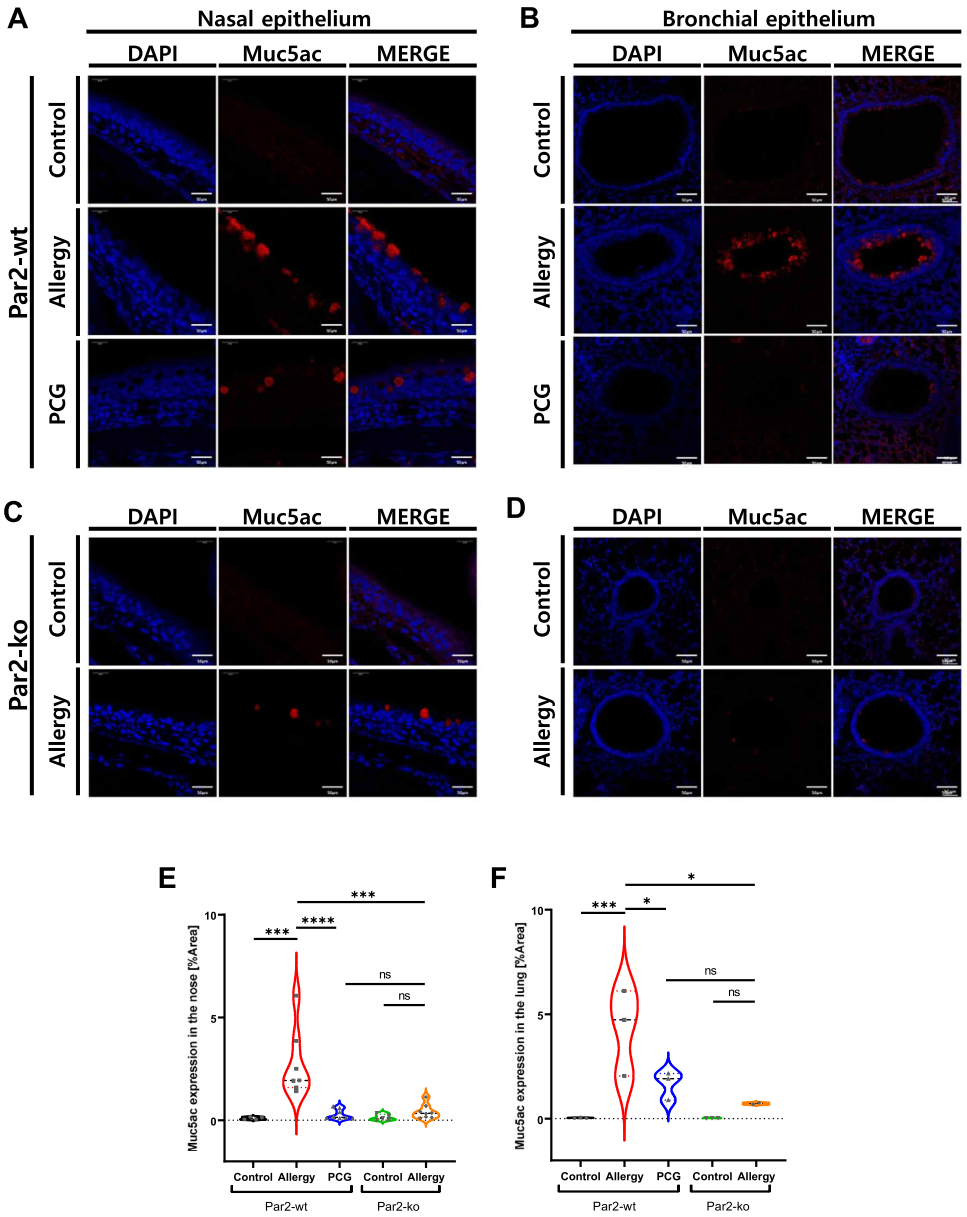

FIGURE 6 | Muc5ac expression in nasal and bronchial epithelium in the mouse model. (A) In PAR2-wt mice, the PCG group showed more suppression of Muc5ac expression in nasal epithelium than the allergy group. (B) In PAR2-wt mice, the PCG group showed more suppression of Muc5ac expression in the bronchial epithelium than the allergy group. (C) In PAR2-ko mice, Muc5ac expression in nasal epithelium in the allergy group was similar to that in the control group. (D) In PAR2-ko mice, Muc5ac expression in the bronchial epithelium in the allergy group was similar to that in the control group. (E) Comparison of Muc5ac expression in the nasal epithelium among groups. The PAR2-wt PCG group and the PAR2-ko allergy group showed significantly lower Muc5ac expression than the PAR2-wt allergy group. (F) Comparison of Muc5ac expression in the bronchial epithelium among groups. The PAR2-wt PCG group and the PAR2-ko allergy group showed significantly lower Muc5ac expression than the PAR2-wt allergy group. *Scale bar, 50 μm; Blue, DAPI; Red, Muc5ac.* PAR2, protease-activated receptor 2; PAR2-ko, PAR2 knockout; PAR2-wt, PAR2 wild-type; PCG, punicalagin. *$p < 0.05$; **$p < 0.01$; ***$p < 0.001$; ****$p < 0.0001$; ns $p > 0.05$.

4 | Discussion

Our findings demonstrate that PAR2 plays a central role in orchestrating both Th1 and Th2 inflammatory responses in allergic airways, and its selective inhibition by PCG offers a novel therapeutic approach. PAR2 activation promotes inflammatory responses through multiple signaling cascades, including Mapk pathways (ERK, p-38, and JNK) and NF-κB phosphorylation [18–20]. In airway epithelium, this activation leads to junctional disruptions and barrier dysfunction, initiating the inflammatory cascade [20]. Our results confirm PAR2's role in mediating these pathways and demonstrate PCG's effectiveness in inhibiting these responses. The dual modulatory effect of PCG on inflammatory responses was observed by its suppression of both Th2 and Th1 cytokines. On the Th2 axis, IL-33 and TSLP were abundantly secreted from HNE cells by HDM stimulation, representing key initiators of allergic inflammation [21]. Simultaneously, on the Th1 axis, HDM stimulation induced significant TNF-α, IL-7, and

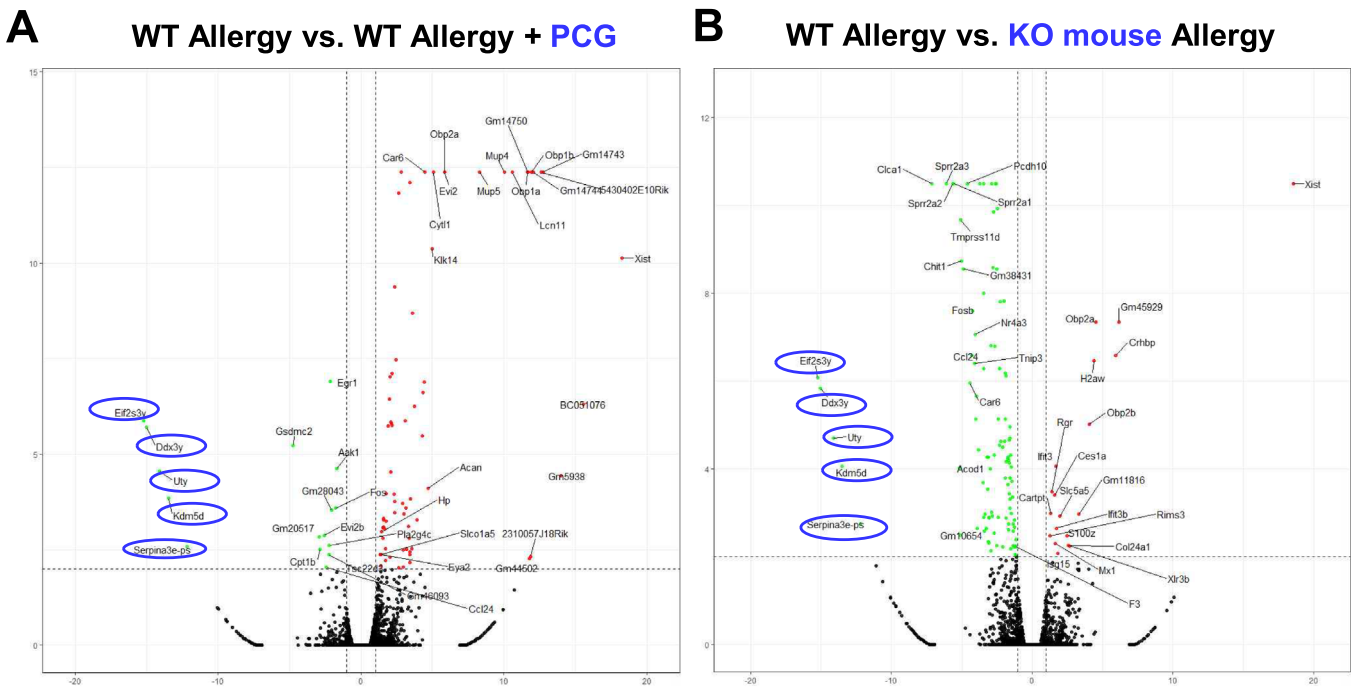

FIGURE 7 | Volcano plots illustrating gene regulation following PAR2 inhibition in the nose and lungs. (A) In allergic rhinitis (AR) mice treated with PCG, *Eif2s3y*, *Ddx3y*, *Uty*, *Kdm5d*, and *Serpina3e-ps* were the most significantly downregulated genes in nasal tissue. (B) In AR mice with PAR2 knockout (PAR2-ko), the same five genes were the most significantly downregulated compared with wild-type (wt) AR mice. (C) In asthma mice treated with PCG, the top five significantly suppressed genes in the lungs were *Eif2s3y*, *Ddx3y*, *Uty*, *Kdm5d*, and *Gm42031*. (D) Asthma mice with PAR2-ko exhibited the same top five significantly suppressed genes compared with wt asthma mice. PCG, punicalagin.

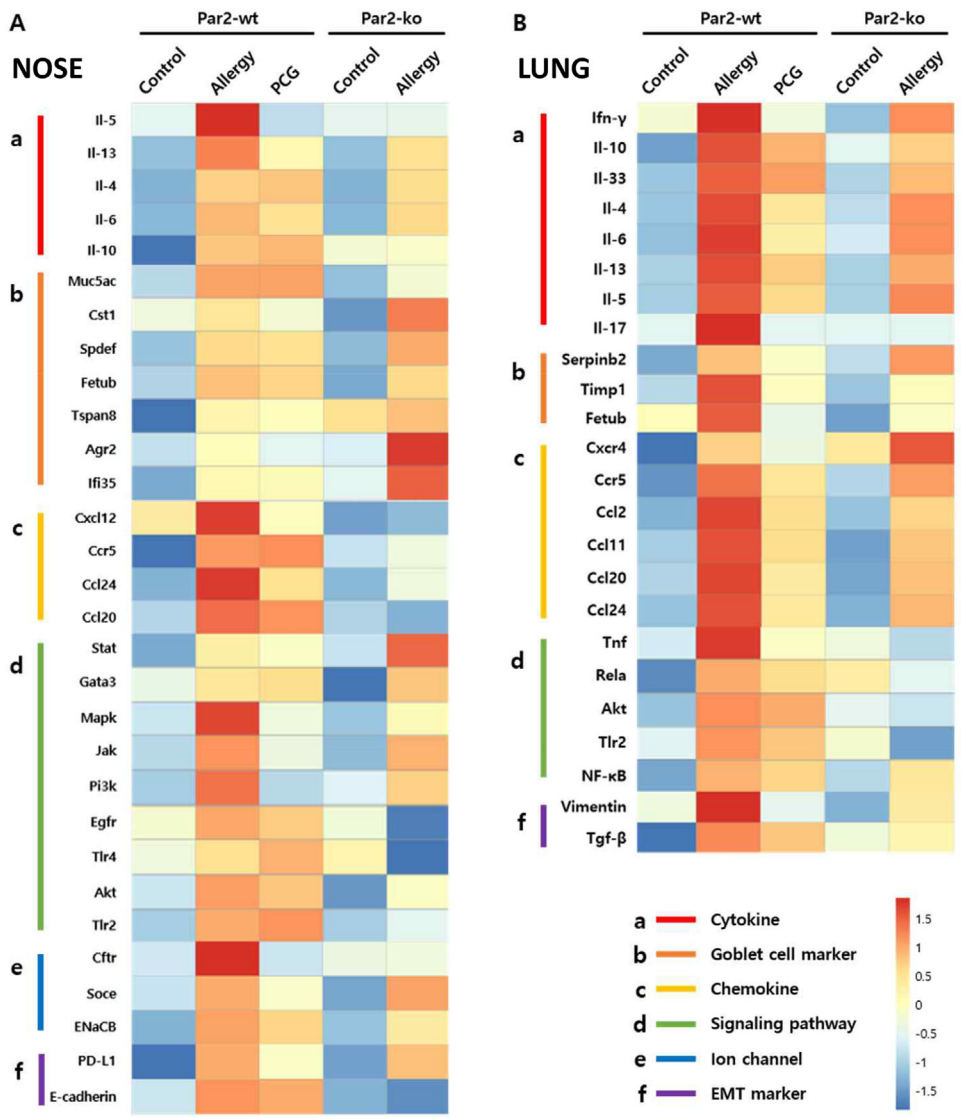

FIGURE 8 | Heatmap displaying differential gene expression in nasal (A) and lung (B) tissues. Gene expression levels are categorized and represented for Th2 cytokines, goblet cell markers [24], chemokines, signaling pathways, ion channels, and markers of epithelial–mesenchymal transition (EMT). IL, interleukin; PAR2, protease-activated receptor 2; PAR2-ko, PAR2 knockout; PAR2-wt, PAR2 wild-type; PCG, punicalagin.

IL-6 production (Figure 2A,B) [22]. PCG effectively suppressed both sets of inflammatory mediators, demonstrating its comprehensive anti-inflammatory capabilities. This dual suppression of Th1 and Th2 pathways distinguishes PCG from traditional therapeutic approaches that typically target mainly Th2 inflammatory response.

The role of PAR2 inhibition in allergic inflammation is further suggested by our findings of IgE responses. PAR2 inhibition effectively suppressed total and HDM-specific serum IgE levels (Figure 3B,C), suggesting its role in preventing allergic sensitization. This result aligns with previous studies showing PAR2's involvement in HDM-induced IgE responses and allergic sensitization in mice [23, 24]. The ability to block this initial sensitization step through PAR2 represents a potentially therapeutic strategy.

Our PAR2-ko mouse studies validate PAR2's role in allergic airway disease. Although PAR2-ko mice have been previously used to study various inflammatory conditions [25–27], our focus on HDM-induced inflammation offers particular clinical relevance. Unlike ovalbumin models with limited human disease relevance, HDM represents a common real-world allergen [28–30]. The attenuation of asthma and rhinitis phenotypes in both PAR2-ko mice and PCG-treated wt mice demonstrates the therapeutic potential of PAR2 inhibition in our study.

It is well known that PCG possesses antioxidant properties, which may contribute to its anti-inflammatory effects. Although a control compound with comparable antioxidant activity but devoid of PAR2-inhibitory effects was not included in this study, we observed that PCG-treated allergic mice exhibited anti-inflammatory responses and gene expression patterns similar

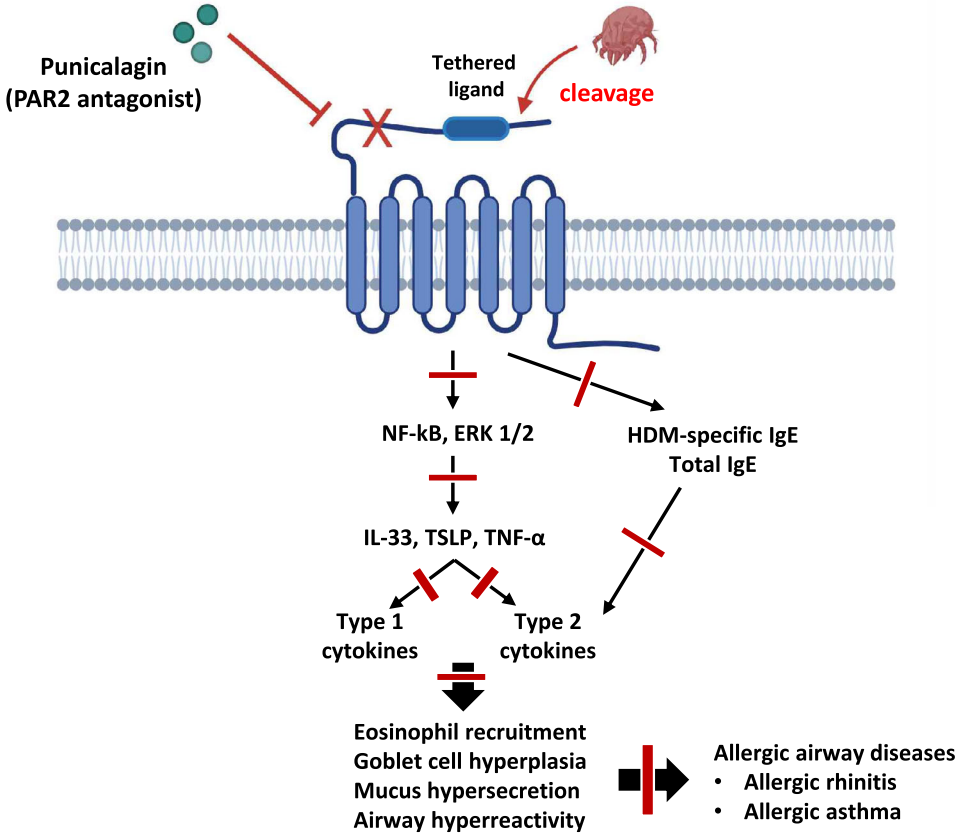

FIGURE 9 | Mechanism of the PAR2 inhibitory effect on allergic airway inflammation. Punicalagin prevents HDM protease-mediated cleavage of the PAR2 receptor's tethered ligand, thereby inhibiting downstream signaling. This inhibition suppresses both NF-κB and ERK1/2 pathways, reducing the production of key inflammatory mediators (IL-33, TSLP, TNF-α) that drive both Type 1 and Type 2 cytokine responses. Consequently, PAR2 inhibition attenuates the phenotype of allergic rhinitis and allergic asthma. HDM, house dust mite; IgE, immunoglobulin E; IL, interleukin.

to those of PAR2-ko mice. As shown in Figure 7, the five most significantly downregulated genes in bronchial tissue were consistently observed in both PCG-treated and PAR2-ko mice. These findings suggest that, although the contribution of PCG's antioxidant activity cannot be entirely ruled out, the suppression of allergic inflammation is likely mediated, at least in large part, through PAR2 inhibition.

Here, we did not perform direct binding assays between PCG and PAR2. However, our previous study suggests that PCG is approximately 30-fold more selective for PAR2 over PAR1 [10]. To support its selectivity further, we performed molecular docking simulations using the crystal structure of PAR2 (PDB ID: 5NDZ) and AutoDock Vina. The docking results indicated that PCG interacts with several key residues in the extracellular domain of PAR2, including Lys213, Thr215, Leu230, Gln233, and Gly318 (Figure S3). These residues are located near the ligand-binding pocket, suggesting a likely mode of selective interaction between PCG and PAR2.

HDM allergens are known to activate multiple pattern recognition and epithelial receptors, including Tlr4, C-type lectin receptors, and egfr [31–33]. However, our findings indicate that PAR2 functions as the predominant mediator of HDM-induced ERK1/2 and NF-κB activation in HNE cells. Pharmacological inhibition of PAR2 using AZ3451, a selective and potent antagonist, markedly suppressed HDM-induced phosphorylation of ERK1/2 and p65, highlighting the central role of PAR2-driven signaling in this context (Figure S1). Although we do not exclude the involvement of other receptor pathways, these results strongly support the interpretation that PAR2 serves as a principal upstream regulator of HDM-induced inflammatory signaling in the airway epithelium.

Developing effective PAR2 antagonists has been a significant challenge. Previous attempts, including ENMD-1068, showed promise but were limited because of low specificity and high IC_{50} values (5 mM) [34, 35]. Other compounds such as AZ8838 and I-191 also lacked selectivity for PAR2 [7, 36]. C391 showed promise in acute allergen challenge models [37], but PCG represents an advance in selectivity and potency [10]. As a natural compound, PCG demonstrates high selectivity for PAR2 with an IC_{50} below 3 μM, suggesting potential therapeutic advantages [10].

Our comprehensive approach, utilizing both primary HNE cells and mouse models, provides strong evidence for PCG's therapeutic potential in allergic respiratory diseases. PCG's mechanism of action, preventing allergen-induced cleavage of PAR2's N-terminus, effectively blocks the initiating step of allergic inflammation. Our mouse model was made under isoflurane

sedation during all intranasal HDM challenges. This anesthetized administration method ensures that the HDM solution effectively reaches both the upper and lower airways, allowing for the simultaneous development of AR and asthma phenotypes. This technique enhances our model's relevance by imitating the unified airway concept seen in human patients who often have both conditions simultaneously. The parallel suppression of inflammation in both nasal and bronchial tissues is particularly relevant given the frequent co-occurrence of asthma and rhinitis. The similar inflammatory profiles observed between PCG-treated wt mice and PAR2-ko mice further validate PCG's specificity and therapeutic potential. This study establishes PCG as a promising therapeutic candidate for allergic airway diseases through its selective inhibition of PAR2 and subsequent modulation of Th1 and Th2 responses (Figure 9). Future studies should focus on optimizing PCG's therapeutic application and investigating potential synergies with existing treatments.

Author Contributions

Miran Kang, Hyung-Ju Cho, and Wan Namkung were involved in study design, experiments, data analysis, and writing and revising the manuscript. Hyejin Jeon, Su-Myeong Jang, Yohan Seo and Ju Hee Seo were involved in experiments and data analysis. Chang-Hoon Kim and Yeonsu Jeong were involved in reviewing and discussing data. All authors were involved in data collection and reviewing and revising the manuscript.

Conflicts of Interest

The authors declare no conflicts of interest.

References

1. A. Heffernan, A. Shafiee, T. Chan, S. Sparanese, and A. Thamboo, "Non-Type 2 and Mixed Inflammation in Chronic Rhinosinusitis and Lower Airway Disease," *Laryngoscope* 134, no. 3 (2024): 1005–1013, https://doi.org/10.1002/lary.30992.

2. F.-L. Huang, E.-C. Liao, and S.-J. Yu, "House Dust Mite Allergy: Its Innate Immune Response and Immunotherapy," *Immunobiology* 223, no. 3 (2018): 300–302.

3. K. J. Stebbins, A. R. Broadhead, L. D. Correa, et al., "Therapeutic Efficacy of AM156, a Novel Prostanoid DP2 Receptor Antagonist, in Murine Models of Allergic Rhinitis and House Dust Mite-Induced Pulmonary Inflammation," *European Journal of Pharmacology* 638, no. 1–3 (2010): 142–149.

4. D.-Y. Wang, "Risk Factors of Allergic Rhinitis: Genetic or Environmental?," *Therapeutics and Clinical Risk Management* 1, no. 2 (2005): 115–123.

5. J. W. Mims, *Asthma: Definitions and Pathophysiology* (Wiley Online Library, 2015).

6. N. R. Lee, S. Y. Baek, A. Gu, et al., "House Dust Mite Allergen Suppresses Neutrophil Apoptosis by Cytokine Release via PAR2 in Normal and Allergic Lymphocytes," *Immunologic Research* 64, no. 1 (2016): 123–132.

7. Y. Jiang, M.-K. Yau, J. Lim, et al., "A Potent Antagonist of Protease-Activated Receptor 2 That Inhibits Multiple Signaling Functions in Human Cancer Cells," *Journal of Pharmacology and Experimental Therapeutics* 364, no. 2 (2018): 246–257.

8. P. G. McMenamin, "The Distribution of Immune Cells in the Uveal Tract of the Normal Eye," *Eye (London, England)* 11, no. 2 (1997): 183–193.

9. A. S. Rothmeier and W. Ruf, *Protease-Activated Receptor 2 Signaling in Inflammation* (Springer, 2012).

10. Y. Seo, C. H. Mun, S.-H. Park, et al., "Punicalagin Ameliorates Lupus Nephritis via Inhibition of PAR2," *International Journal of Molecular Sciences* 21, no. 14 (2020): 4975.

11. A. Jairaman, M. Yamashita, R. P. Schleimer, and M. Prakriya, "Store-Operated Ca^{2+} Release-Activated Ca^{2+} Channels Regulate PAR2-Activated Ca^{2+} Signaling and Cytokine Production in Airway Epithelial Cells," *Journal of Immunology* 195, no. 5 (2015): 2122–2133, https://doi.org/10.4049/jimmunol.1500396.

12. H. J. Cho, J. Y. Choi, Y. M. Yang, et al., "House Dust Mite Extract Activates Apical Cl(-) Channels Through Protease-Activated Receptor 2 in human Airway Epithelia," *Journal of Cellular Biochemistry* 109, no. 6 (2010): 1254–1263, https://doi.org/10.1002/jcb.22511.

13. I. F. Abdullaev, J. M. Bisaillon, M. Potier, J. C. Gonzalez, R. K. Motiani, and M. Trebak, "Stim1 and Orai1 Mediate CRAC Currents and Store-Operated Calcium Entry Important for Endothelial Cell Proliferation," *Circulation Research* 103, no. 11 (2008): 1289–1299.

14. S. Boitano, A. N. Flynn, C. L. Sherwood, et al., "*Alternaria alternata* Serine Proteases Induce Lung Inflammation and Airway Epithelial Cell Activation via PAR2," *American Journal of Physiology-Lung Cellular and Molecular Physiology* 300, no. 4 (2011): L605–L614.

15. H. J. Cho, H. J. Lee, S. C. Kim, et al., "Protease-Activated Receptor 2-Dependent Fluid Secretion From Airway Submucosal Glands by House Dust Mite Extract," *Journal of Allergy and Clinical Immunology* 129, no. 2 (2012): 529–535, https://doi.org/10.1016/j.jaci.2011.11.024.

16. L. Yu and J. Li, "Punicalagin Attenuated Allergic Airway Inflammation via Regulating IL4/IL-4Ralpha/STAT6 and Notch- GATA3 Pathways," *Acta Pharmaceutica* 72, no. 4 (2022): 561–573, https://doi.org/10.2478/acph-2022-0038.

17. B. Steelant, P. Wawrzyniak, K. Martens, et al., "Blocking Histone Deacetylase Activity as a Novel Target for Epithelial Barrier Defects in Patients With Allergic Rhinitis," *Journal of Allergy and Clinical Immunology* 144, no. 5 (2019): 1242–1253.

18. H. Inaba, H. Sugita, M. Kuboniwa, et al., "*Porphyromonas gingivalis* Promotes Invasion of Oral Squamous Cell Carcinoma Through Induction of Pro MMP 9 and Its Activation," *Cellular Microbiology* 16, no. 1 (2014): 131–145.

19. T. Kanke, S. R. Macfarlane, M. J. Seatter, et al., "Proteinase-Activated Receptor-2-Mediated Activation of Stress-Activated Protein Kinases and Inhibitory Kappa B Kinases in NCTC 2544 Keratinocytes," *Journal of Biological Chemistry* 276, no. 34 (2001): 31657–31666, https://doi.org/10.1074/jbc.M100377200.

20. Y. J. Wang, S. J. Yu, J. J. Tsai, C. H. Yu, and E. C. Liao, "Antagonism of Protease Activated Receptor-2 by GB88 Reduces Inflammation Triggered by Protease Allergen Tyr-p3," *Frontiers in Immunology* 12 (2021): 557433, https://doi.org/10.3389/fimmu.2021.557433.

21. F. Roan, K. Obata-Ninomiya, and S. F. Ziegler, "Epithelial Cell-Derived Cytokines: More Than Just Signaling the Alarm," *Journal of Clinical Investigation* 129, no. 4 (2019): 1441–1451, https://doi.org/10.1172/JCI124606.

22. S. H. Shin, M. K. Ye, D. W. Lee, M. H. Chae, and B. D. Han, "Nasal Epithelial Cells Activated With Alternaria and House Dust Mite Induce Not Only Th2 but Also Th1 Immune Responses," *International Journal of Molecular Sciences* 21, no. 8 (2020): 2693, https://doi.org/10.3390/ijms21082693.

23. S. Post, I. H. Heijink, A. H. Petersen, H. G. de Bruin, A. J. van Oosterhout, and N. MC, "Protease-Activated Receptor-2 Activation Contributes to House Dust Mite-Induced IgE Responses in Mice," *PLoS ONE* 9, no. 3 (2014): e91206, https://doi.org/10.1371/journal.pone.0091206.

24. C. E. Davidson, M. Asaduzzaman, N. G. Arizmendi, et al., "Proteinase-Activated Receptor-2 Activation Participates in Allergic Sensitization to House Dust Mite Allergens in a Murine Model," *Clinical and*

Experimental Allergy 43, no. 11 (2013): 1274–1285, https://doi.org/10.1111/cea.12185.

25. M. K. Yau, J. Lim, L. Liu, and D. P. Fairlie, "Protease Activated Receptor 2 (PAR2) Modulators: A Patent Review (2010–2015)," *Expert Opinion on Therapeutic Patents* 26, no. 4 (2016): 471–483, https://doi.org/10.1517/13543776.2016.1154540.

26. F. Schmidlin, S. Amadesi, K. Dabbagh, et al., "Protease-Activated Receptor 2 Mediates Eosinophil Infiltration and Hyperreactivity in Allergic Inflammation of the Airway," *Journal of Immunology* 169, no. 9 (2002): 5315–5321, https://doi.org/10.4049/jimmunol.169.9.5315.

27. T. Takizawa, M. Tamiya, T. Hara, et al., "Abrogation of Bronchial Eosinophilic Inflammation and Attenuated Eotaxin Content in Protease-Activated Receptor 2-Deficient Mice," *Journal of Pharmacological Sciences* 98, no. 1 (2005): 99–102, https://doi.org/10.1254/jphs.scz050138.

28. N. G. Arizmendi, M. Abel, K. Mihara, et al., "Mucosal Allergic Sensitization to Cockroach Allergens Is Dependent on Proteinase Activity and Proteinase-Activated Receptor-2 Activation," *Journal of Immunology* 186, no. 5 (2011): 3164–3172, https://doi.org/10.4049/jimmunol.0903812.

29. J. D. de Boer, C. van't Veer, I. Stroo, et al., "Protease-Activated Receptor-2 Deficient Mice Have Reduced House Dust Mite-Evoked Allergic Lung Inflammation," *Innate Immunity* 20, no. 6 (2014): 618–625.

30. J. Daan de Boer, J. J. Roelofs, A. F. de Vos, et al., "Lipopolysaccharide Inhibits Th2 Lung Inflammation Induced by House Dust Mite Allergens in Mice," *American Journal of Respiratory Cell and Molecular Biology* 48, no. 3 (2013): 382–389, https://doi.org/10.1165/rcmb.2012-0331OC.

31. H. Hammad, M. Chieppa, F. Perros, M. A. Willart, R. N. Germain, and B. N. Lambrecht, "House Dust Mite Allergen Induces Asthma via Toll-Like Receptor 4 Triggering of Airway Structural Cells," *Nature Medicine* 15, no. 4 (2009): 410–416, https://doi.org/10.1038/nm.1946.

32. T. Ito, K. Hirose, A. Norimoto, et al., "Dectin-1 Plays an Important Role in House Dust Mite-Induced Allergic Airway Inflammation Through the Activation of CD11b+ Dendritic Cells," *Journal of Immunology* 198, no. 1 (2017): 61–70, https://doi.org/10.4049/jimmunol.1502393.

33. I. H. Heijink, A. van Oosterhout, and A. Kapus, "Epidermal Growth Factor Receptor Signalling Contributes to House Dust Mite-Induced Epithelial Barrier Dysfunction," *European Respiratory Journal* 36, no. 5 (2010): 1016–1026, https://doi.org/10.1183/09031936.00125809.

34. A. Nadeem, N. O. Alharbi, H. Vliagoftis, M. Tyagi, S. F. Ahmad, and M. M. Sayed-Ahmed, "Proteinase Activated Receptor-2-Mediated Dual Oxidase-2 Up-Regulation Is Involved in Enhanced Airway Reactivity and Inflammation in a Mouse Model of Allergic Asthma," *Immunology* 145, no. 3 (2015): 391–403.

35. E. B. Kelso, J. C. Lockhart, T. Hembrough, et al., "Therapeutic Promise of Proteinase-Activated Receptor-2 Antagonism in Joint Inflammation," *Journal of Pharmacology and Experimental Therapeutics* 316, no. 3 (2006): 1017–1024, https://doi.org/10.1124/jpet.105.093807.

36. A. J. Kennedy, L. Sundström, S. Geschwindner, et al., "Protease-Activated Receptor-2 Ligands Reveal Orthosteric and Allosteric Mechanisms of Receptor Inhibition," *Communications Biology* 3, no. 1 (2020): 1–13.

37. C. M. Rivas, M. C. Yee, K. J. Addison, et al., "Proteinase-Activated Receptor-2 Antagonist C391 Inhibits Alternaria-Induced Airway Epithelial Signalling and Asthma Indicators in Acute Exposure Mouse Models," *British Journal of Pharmacology* 179, no. 10 (2022): 2208–2222, https://doi.org/10.1111/bph.15745.

Supporting Information

Additional supporting information can be found online in the Supporting Information section.

Figure S1: HDM induces PAR2-mediated phosphorylation of ERK1/2 and p65 in human nasal epithelial cells. (A, B) Western blot analysis of phospho-ERK1/2 (p-ERK1/2), total ERK1/2 (t-ERK1/2), phosphop65 (p-p65), and total p65 (t-p65) in human nasal epithelial cells. Cells were cultured in serum-free medium for 24 h, then pretreated with 3 μM AZ3451, a potent and selective PAR2 antagonist, for 30 min prior to stimulation with 30 μg/ml HDM (mean ± S.E., $n = 3$). *$p < 0.05$; **$p < 0.01$; ***$p < 0.001$. **Figure S2:** Bulk RNA-seq analysis in nasal and lung tissues of the mouse model Heatmap comparing gene expression in nasal tissue among groups. (B) Heatmap comparing gene expression in lung tissue among groups. **Figure S3:** Predicted molecular interactions between PCG and PAR2 from docking simulations. (A) Predicted binding models of PCG docked to the extracellular domain of PAR2. (B) Close-up view showing PCG interactions with key residues at the predicted binding site of the extracellular domain of PAR2. (C) Alternative close-up view of PCG binding to PAR2, highlighting key residue interactions. **Table S1:** Primer sequence information used to identify the genotype of protease-activated receptor 2 transgenic mice.